Synthesis and Characterization of Hybrid Membranes Using Poly(vinyl alcohol) and Tetraethylorthosilicate for the Pervaporation Separation of Water–Isopropanol Mixtures

Srikant S. Kulkarni, Arjumand A. Kittur, Mrityunjaya I. Aralaguppi, Mahadevappa Y. Kariduraganavar

Department of Chemistry and Center of Excellence in Polymer Science, Karnatak University, Dharwad 580003, India

Received 30 July 2003; accepted 8 March 2004
DOI 10.1002/app.21088
Published online in Wiley InterScience (www.interscience.wiley.com).

ABSTRACT: Hybrid membranes were prepared using poly(vinyl alcohol) (PVA) and tetraethylorthosilicate (TEOS) via hydrolysis and cocondensation reaction for the pervaporation separation of water-isopropanol mixtures. The resulting membranes were characterized by Fourier transform infrared spectroscopy, wide-angle X-ray diffraction, and differential scanning calorimetry. The glass transition temperature of these membranes varied from 100 to 120°C with increasing TEOS content. Effects of crosslinking density and feed compositions on the pervaporation performances of the membranes were studied. The membrane containing 1.5:1 mass ratio of TEOS to PVA gave the highest separation selectivity of 900 at 30°C for 10 mass % of water in the feed mixture. It was found that the separation selectivity and permeation flux data are strongly dependent on the water composition of the feed and operating temperature. However, the membrane with the highest crosslinking density showed unusual pervaporation properties. The overall activation energy values were calculated using the Arrhenius-type equation. The activation energy values for the permeation and diffusion varied from 49.18 to 64.96 and 55.13 to 67.31 kJ/mol, respectively. Pervaporation data have also been explained on the basis of thermodynamic quantities.

Key words: poly(vinyl alcohol); TEOS; hybrid membranes; pervaporation; selectivity; activation energy

INTRODUCTION

Pervaporation (PV) is an energy-efficient, membrane-based process, a combination of evaporation and permeation, and is considered an attractive alternative for many separation processes. The process, which requires only low temperature and pressure, has cost and performance advantages compared to conventional separation for azeotropic mixtures,[1,2] close boiling components,[3–5] and isomeric mixtures.[6] In the PV process, the liquid mixture is maintained at atmospheric pressure on the feed side of the membrane and the permeate is removed on the other side as a vapor, because of a low vapor pressure existing on the downstream side. This low vapor pressure can be achieved by employing a carrier gas or using a vacuum pump. The partial downstream pressure must at least be lower than the saturation pressure.

Isopropanol has been widely used in semiconductor and liquid crystal display industries as a water-removing agent.[7] Used isopropanol can be recycled by several methods, including pervaporation processes. Water and isopropanol form an azeotrope at 85.3 mass % of isopropanol concentration. The selective separation of water from aqueous mixtures of isopropanol or the dehydration of isopropanol can be carried out with different membranes, which contain polar groups, either in the backbone or as pendent moieties. For the dehydration of such a mixture, poly(vinyl alcohol) (PVA) and PVA-based membranes[8,9] have been used extensively. PVA is the primary material from which the commercial Gesellshaft Fur Trenntechnik membranes are fabricated and has been studied intensively in pervaporation because of its excellent film forming, high hydrophilicity due to –OH groups as pendant moieties, and chemical-resistant properties.[10–12] On the contrary, PVA has poor stability at higher water concentrations, and hence selectivity decreases remarkably.[13] To improve the stability of PVA at higher water concentration, two methods have been suggested:[14] crystallization and

CEPS Communication No. 50.

Correspondence to: M. Y. Kariduraganavar (mahadevappak@yahoo.com).

Contract grant sponsor: Department of Science and Technology, New Delhi, India; contract grant number: SP/S1/H-31/2000.

crosslinking. Although PVA membranes with crystallization pretreatment can be used at higher water concentrations, they are still unstable at higher temperatures.[13] Therefore, crosslinking seems to be the best method to improve the stability against water and organic solvents at higher temperatures. Many crosslinking methods for PVA membrane applications are being used in the literature.[15–20] In addition, either chemical or physical incorporation of some of the inorganic species like silica, zirconia, and titania into the polymer matrix enhances the properties such as flexibility and toughness of the resulting membranes.[21–23]

The present work represents the synthesis of PVA-based hybrid membranes, involving the hydrolysis and cocondensation of TEOS precursors with the reactive –OH groups of PVA under acidic conditions.[24] The TEOS content with respect to PVA was varied to improve the membrane's performance. The resulting membranes were tested for PV separation of water–isopropanol mixtures at 30, 40, and 50°C. The overall activation energies for permeation and diffusion were calculated using the Arrhenius-type equation.

EXPERIMENTAL

Materials

Poly(vinyl alcohol) ($\bar{M}_w$~125,000), isopropanol, and hydrochloric acid were purchased from S. D. Fine Chemicals Ltd. (Mumbai, India). Tetraethylorthosilicate (TEOS) was procured from E. Merck Ltd. (Mumbai, India). All chemicals are of reagent grade and were used without further purification. Water was deionized and distilled before use.

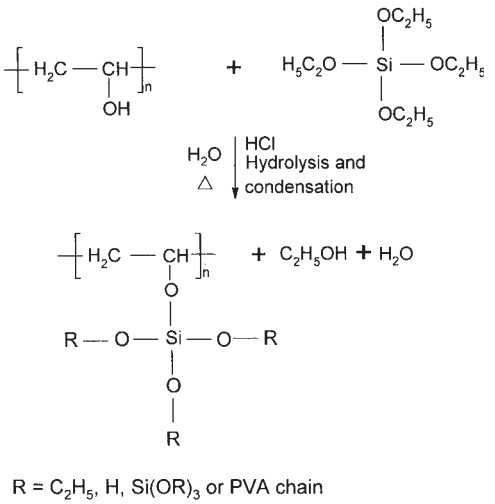

Figure 1 Scheme for the synthesis of PVA-based hybrid membrane.

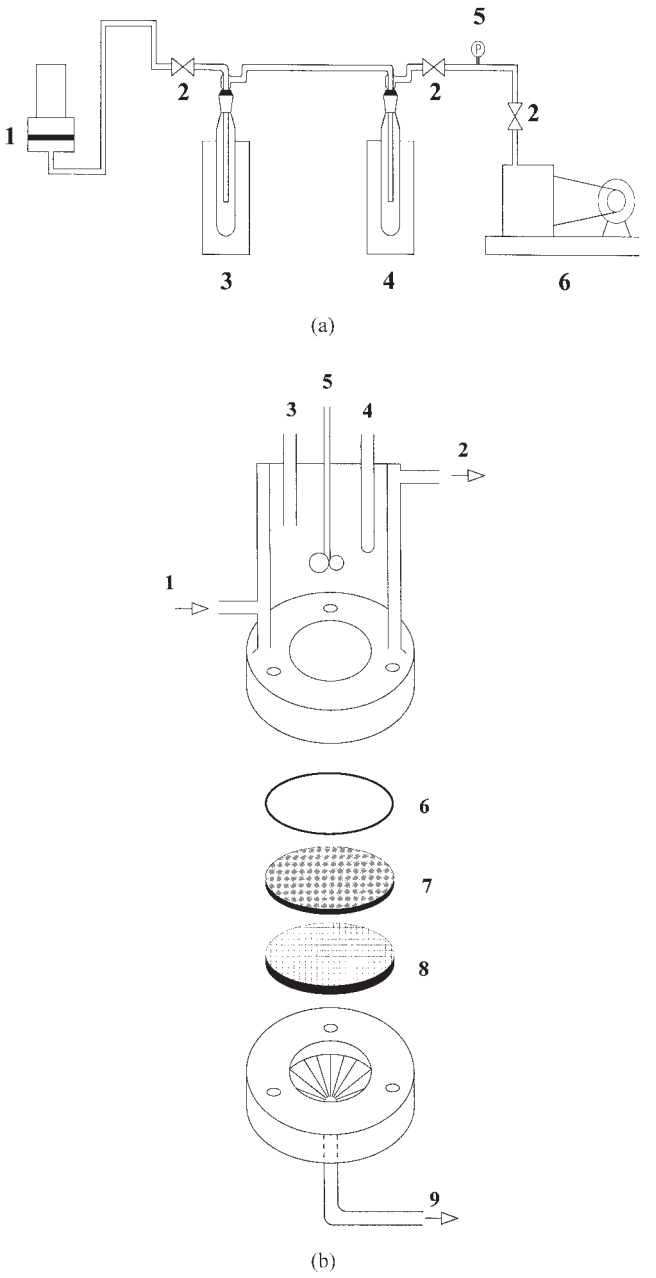

Figure 2 (A) Schematic representation of pervaporation apparatus: (1) pervaporation cell; (2) vacuum control valve; (3) permeate cold trap; (4) moisture cold trap; (5) pressure sensor; (6) vacuum pump. (B) Schematic diagram of pervaporation cell: (1) water inlet; (2) water outlet; (3) feed inlet; (4) thermometer jacket; (5) stirrer; (6) o-ring; (7) membrane; (8) sintered disk; (9) permeate outlet.

Membrane preparation

Poly(vinyl alcohol) (4 g) was dissolved in 100 mL of deareated-distilled water at 60°C. The hot solution was filtered and a known amount of TEOS and 1 mL of concentrated HCl as catalyst were added to the filtrate. The solution was stirred overnight at the same temperature and the resulting homogeneous solution

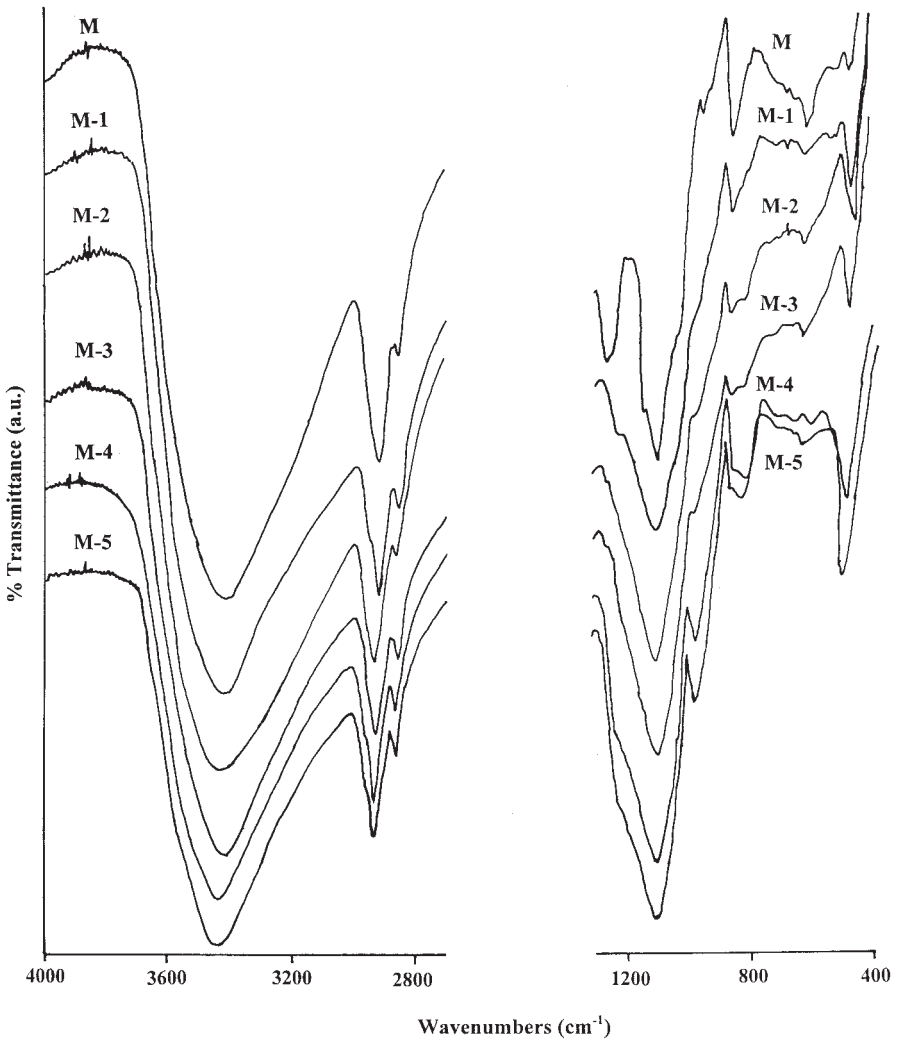

Figure 3 (A) FTIR spectra of pure PVA and its hybrid membranes: (M) 0 mass ratio; (M-1) 0.25 mass ratio; (M-2) 0.5 mass ratio (M-3) 1.0 mass ratio; (M-4) 1.5 mass ratio; and (M-5) 2.0 mass ratio of TEOS. (B) FTIR spectra of pure PVA and its unreacted mixtures: (X) 0 mass ratio; (X-1) 0.25 mass ratio; (X-2) 0.5 mass ratio (X-3) 1.0 mass ratio; (X-4) 1.5 mass ratio; and (X-5) 2.0 mass ratio of TEOS.

was cast onto a glass plate with the aid of a casting knife. The membranes were allowed to dry at room temperature for 2–3 days and the completely dried membranes were subsequently peeled off. The mass ratio of TEOS to PVA was varied at 0.25, 0.5, 1.0, 1.5, and 2, and the resulting homogenous hybrid membranes were designated M-1, M-2, M-3, M-4, and M-5, respectively. These correspond to the molar ratios of TEOS and PVA based on the number of hydrolysable OC_2H_5 groups of TEOS and –OH groups of PVA are 0.21, 0.42, 0.84, 1.27, and 1.69, respectively. The thickness of these membranes was measured at different points using a Peacock dial thickness gauge (Model G, Ozaki MFG. Co. Ltd., Japan) with an accuracy of ±5 μm and the average thickness was used for calculation. The scheme for the synthesis of PVA-based hybrid membranes is illustrated in Figure 1.

Fourier transform infrared (FTIR) spectroscopy

The reaction between PVA and TEOS was confirmed using an FTIR spectrometer (Nicolet, Impact- 410, USA). Membrane samples were ground well to make KBr pellets under hydraulic pressure of 400 kg/cm^2 and the spectra were recorded in the range of 400-4000 cm^{-1}.

Wide-angle X-ray diffraction (WAXD)

The morphology of the pure PVA and its hybrid membranes was studied at room temperature using a Bruker D-8 advanced wide-angle X-ray diffractometer. The X-ray source was nickel-filtered Cu-Kα radiation (40 KV, 30 mA). Dried membranes of uniform thickness (~45 μm) were mounted on a sample holder and scanned in the reflection mode at an angle 2θ over a range from 5 to 45° at a speed of 8° per min.

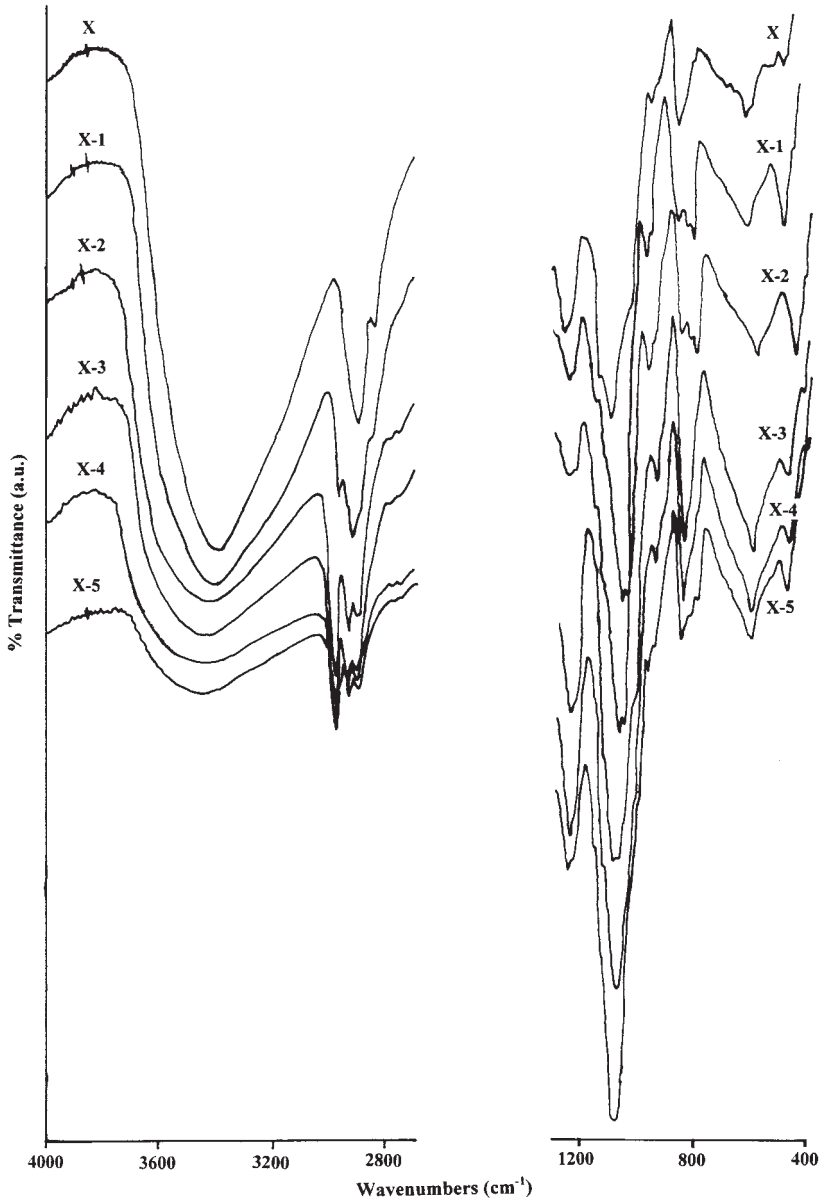

Figure 3 (*Continued from the previous page*)

Differential scanning calorimetry (DSC)

Thermal properties of the pure PVA and its hybrid membranes were measured using a differential scanning calorimeter (Stanton, Redcroff DSC 1500). Sample weights ranged from 5 to 8 mg and were heated from ambient to 300°C at a heating rate of 10°C/min. The intercept point of the slopes was taken as the glass transition temperature (T_g).

Pervaporation experiments

PV experiments were performed using an indigenously designed apparatus shown in Figure 2A and B. The effective surface area of the membrane in contact with the feed mixture is 37.4 cm^2 and the capacity of the feed compartment is about 250 cm^3. The vacuum in the downstream side of the apparatus was maintained (10 Torr) in all experiments using a two-stage vacuum pump (Toshniwal, Chennai, India). The water composition in the feed mixture varied from 10 to 90 mass %. The test membrane was allowed to equilibrate for about 2 h in the feed compartment before the PV experiment was performed with the known volume of feed mixture. After a steady state was attained, the permeate was collected in trap immersed in the liquid nitrogen on the downstream side and experiments were carried out at 30, 40, and 50°C. The flux was calculated by weighing the permeate and its composition was estimated by measuring the refractive index of the mixture within an accuracy of ±0.0001

units using Abbe's refractometer (Atago-3T, Japan) and by comparing it with a standard graph, which was established with the known compositions of water–isopropanol mixtures.

From the PV data, separation performances of the membranes were assessed in terms of total flux (J_p), separation selectivity (α_{sep}), and pervaporation separation index (PSI) and these were calculated, respectively, using the equations

$$J_p = \frac{W_p}{A \cdot t} \quad (1)$$

$$\alpha_{sep} = \frac{P_w / P_{IPA}}{F_w / F_{IPA}} \quad (2)$$

$$PSI = J_p(\alpha_{sep} - 1). \quad (3)$$

Here, W_p is the mass of permeate (g); A is the area of the membrane in contact with the feed mixture (m^2); t is the permeation time (h); P_w and P_{IPA} are the mass percentage of water and isopropanol in the permeate, respectively. F_w and F_{IPA} are, respectively, the mass percentage of water and isopropanol in the feed. The results of permeation for water–isopropanol mixtures during pervaporation were reproducible within the admissible range.

Swelling measurements

The equilibrium sorption experiments were performed in different compositions of water–isopropanol mixtures using an electronically controlled oven (WTB Binder, Germany). The masses of the dry membranes were first determined and these were equilibrated by soaking in different compositions of the mixtures in a sealed vessel at 30°C for 24 h. The swollen membranes were weighed as quickly as possible after careful blotting on a single pan digital microbalance (Mettler, B204-S, Toledo, Switzerland) with a sensitivity of ±0.01 mg. The percentage degree of swelling was calculated as

$$DS(\%) = \left(\frac{W_s - W_d}{W_d}\right) \times 100, \quad (4)$$

where W_s and W_d are the masses of the swollen and dry membranes, respectively.

RESULTS AND DISCUSSION

Membrane characterization

FTIR studies

The incorporation of silicone groups into a PVA matrix was confirmed by IR studies. Figure 3A and B shows the FTIR spectra of pure PVA membrane and its hybrid membranes and unreacted mixture of PVA and TEOS, respectively. A characteristic strong and broad band appearing at around 3400 cm^{-1} in pure PVA spectra (M) corresponds to –OH stretching vibrations of the hydroxyl groups. The intensity of this peak decreased marginally from membrane M-1 to M-5 with increasing TEOS content in the membrane. However, for the unreacted mixtures of PVA and TEOS, the intensity of this peak decreased remarkably and is simply due to the decrease of PVA content (–OH groups) in the mixture with increasing mass ratio of TEOS. This confirms that although the reactive –OH groups of PVA in the membrane are involved in the condensation reaction, still the observed marginal decrease of its intensity from M-1 to M-5 indicates the formation of silanol [$Si(OH)_x$] groups during hydrolysis of TEOS, which add up to the intensity of –OH peak. Further, multiple bands appearing in the spectra (M) at around 1000 to 1100 cm^{-1} are assigned to C–O stretching. The intensity of these bands increased marginally from membrane M-1 to M-5 due to an increase of Si–O groups in the membrane with increasing TEOS content, since the Si–O stretching band appears almost close to the frequency of C–O stretching. However, the intensity of this peak increased significantly for the unreacted mixtures and is simply due to the addition of both C–O and Si–O groups to the C–O groups of PVA with increasing TEOS in the mixture. These explanations suggest the formation of Si–O–C bonds[25,26] in the resulting membrane matrix.

Glass transition temperature (T_g)

The increase of TEOS content in the solution of PVA increased the crosslinking density from membrane M-1 to M-5. This hinders the segmental motion of the chains and thereby increases the chain stiffness owing to a reduction of free volume in the membrane matrix. Besides, the silicone crosslinking groups enhance the toughness of the membranes, as the Si–O bonds are known to be stronger compared to C–C bonds.[27] As a result, the T_g increased exponentially with increasing TEOS content in the membranes, as shown in Figure 4.

X-ray diffraction studies

To study the effect of TEOS on the membrane morphology, X-ray diffraction was employed and the patterns for the PVA and its hybrid membranes are presented in Figure 5. The pure PVA membrane (M) exhibits a typical peak that appeared at $2\theta = 20$ degree[7,28] and thus, it can be assigned to be a mixture of (101) and (200). On the other hand, diffraction patterns of the hybrid membranes show that as the degree of crosslinking density increased from membrane M-1 to M-5, the intensity of the typical peak of PVA de-

creased continuously at around $2\theta = 20$. This reveals that the uncrosslinked PVA membrane exhibits more crystalline domains than those of crosslinked hybrid membranes. From the patterns, it can also be observed that there is a shift in the position of the peaks of hybrid membranes from the pure PVA membrane. This implies that the silanol groups of TEOS crosslink with the reactive –OH groups of PVA in a crystalline domain and results in the compression of the amorphous region, thereby making the structure more compact.[29] This compact structure favors the selective transport.

Swelling study

The swelling of the polymer membrane in some liquids depends on the extent of crosslinking, membrane morphology, interaction between the polymer and penetrants, and the free volume available within the polymer matrix.[30,31] In PV experiments, membrane swelling controls the transport of permeating molecules under the influence of chemical potential gradient. Figure 6 displays the swelling behavior of the PVA-based hybrid membranes in different mass % of water–isopropanol mixtures at 30°C. It is observed that the degree of swelling increased with increasing water concentration in the feed. This behavior is more predominant for the membranes M-1 and M-2 due to lower crosslinking density. For membranes M-3 and M-4, the degree of swelling increased gradually with increasing the water concentration in the feed. This is due to a higher crosslinking density formed between the linear polyethylene segments by the addition of TEOS. However, for the membrane M-5, the degree of swelling is insignificant and did not show any change even after increasing the water concentration in the feed. This clearly indicates that at 2:1 mass ratio of TEOS to PVA, the membrane loses its hydrophilic character considerably due to higher crosslinking density. Therefore, in the present investigation the crosslinking plays a vital role in controlling the swelling behavior of the membranes, which, in turn, is responsible for the rate of permeation of selective molecules through the membranes.

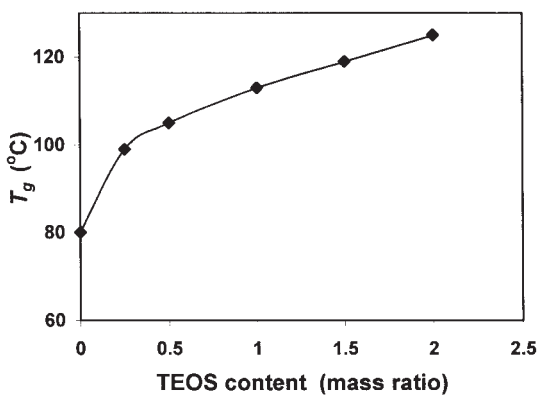

Figure 4 Effect of TEOS on glass transition temperatures.

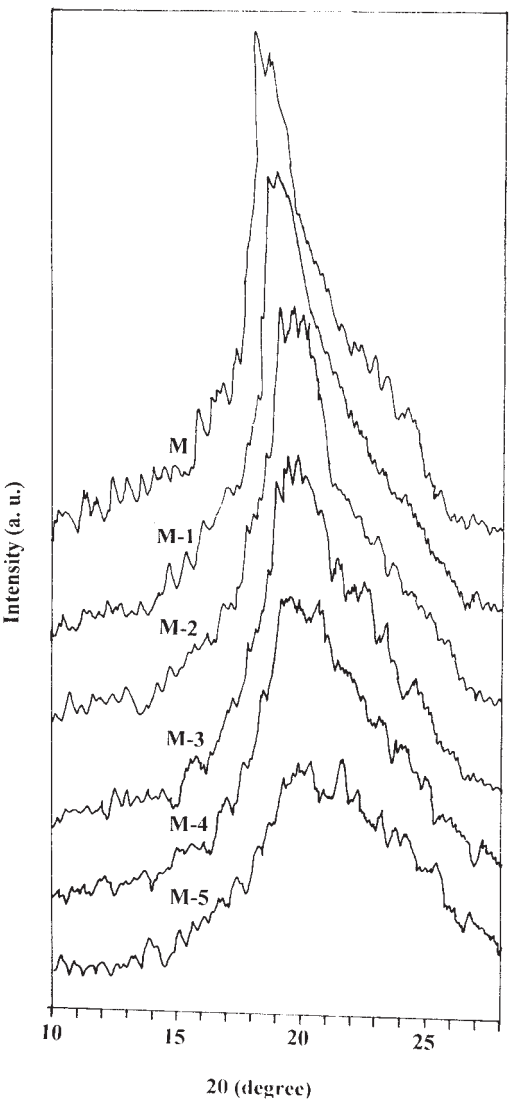

Figure 5 Wide-angle X-ray diffraction patterns of pure PVA and its hybrid membranes: (M) 0 mass ratio; (M-1) 0.25 mass ratio; (M-2) 0.5 mass ratio; (M-3) 1.0 mass ratio; (M-4) 1.5 mass ratio; and (M-5) 2.0 mass ratio of TEOS.

Pervaporation separation index

The PSI is the product of total permeation and separation factor, which characterizes the membrane performances in PV applications. Figure 7 shows the variation of PSI as a function of TEOS content in the membranes for 10 mass % of water in the feed at 30°C. PSI values increase as the crosslinking density increases (M-1 to M-4). However, for membrane M-5, the PSI value decreased. This may be due to a considerable loss of hydrophilic character at higher crosslinking density and, as a result, selectivity re-

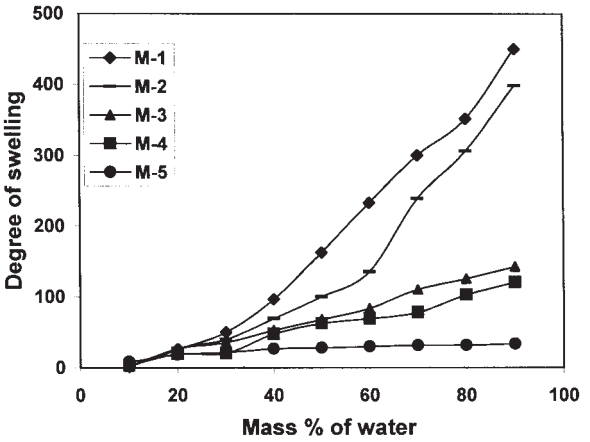

Figure 6 Variation of degree of swelling with different mass % of water in the feed at 30°C for different hybrid membranes.

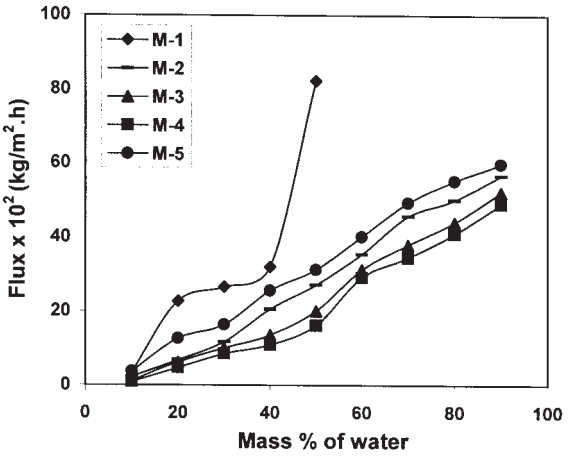

Figure 8 Variation of total pervaporation flux with different mass % of water in the feed at 30°C for different hybrid membranes.

markably decreased toward the water. This suggests that the membranes of the present study showed better performances at higher crosslinking density up to a maximum extent of 1.5:1 mass ratio of TEOS to PVA.

Pervaporation

The pervaporation process combines the evaporation of volatile components of a mixture with their permeation through a polymeric membrane under reduced pressure conditions. It is well accepted that the transport of a volatile substance through a PV membrane involves a sorption step at the membrane upstream face, followed by a diffusion through the dense film and a desorption into the vacuum. Under a high vacuum on the downstream side of the polymer film, the desorption is believed to be a fast step. Thus, the overall separation characteristic of a membrane depends on three crucial factors with regard to the penetrants of the mixture: affinity to the membrane; size of the molecules; and their vapor pressure. The affinity of various volatile molecules toward the membrane could be evaluated from their difference in solubility parameter assessed experimentally by sorption measurements. Uncrosslinked PVA is a glassy polymer with distinct T_m at around 258°C. The pervaporation process of this type of materials is considered diffusion controlled. The permeation rate of the penetrants is highly dependent on their size. The chemically crosslinked PVA with different mass ratios of TEOS resulted in the formation of new hybrid materials with improved pervaporation properties.

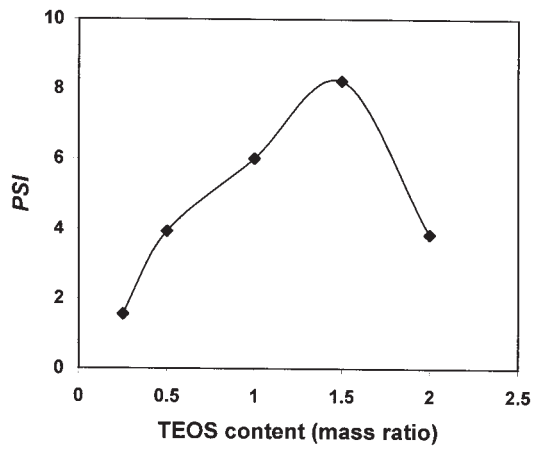

Figure 7 Variation of pervaporation separation index with different mass ratio of TEOS at 30°C for 10 mass % of water in the feed.

Figure 8 shows the total pervaporation flux as a function of water concentration in the feed for the PVA-based hybrid membranes. It is observed that the permeation flux increased linearly for all membranes upon increasing the amount of water content in the feed. This indicates that with increasing water content in the feed the selective interactions between water molecules and the hydrophilic membrane increase. As a result, the total permeation flux increased almost linearly for all membranes through easier diffusion of water molecules. For membrane (M-1), which is less crosslinked, the total permeation flux increased exponentially up to 40 mass % of water in the feed, after which the flux increased greatly from 32 to 82 $\times$ 10^{-2} kg m^{-2} h^{-1}, and beyond 50 mass % the membrane lost its stability due to the attribution of strong affinity between the membrane and water molecules.

On the other hand, the permeation flux decreased from membrane M-1 to M-4 with increasing the crosslinking density. This is because of a significant reduction of free volume followed by a decrease in chain mobility, resulting in less accommodation for the permeate during the diffusion process. In addition,

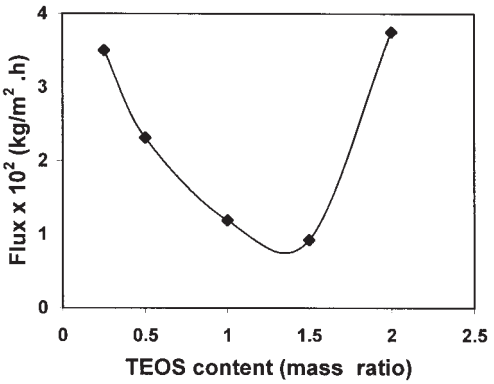

Figure 9 Variation of total pervaporation flux with different mass ratio of TEOS at 30°C for 10 mass % of water in the feed.

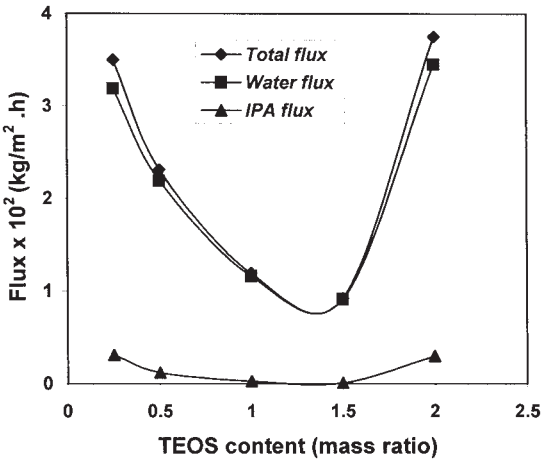

Figure 10 Variation of total flux and fluxes of water and isopropanol with different mass ratio of TEOS at 30°C for 10 mass % of water in the feed.

the hydrophilic character of the membranes reduces from M-1 to M-4 owing to the formation of crosslinks involving –OH molecules between the linear polyethylene units. The results of T_g also indicated that membranes have rigid structures due to a reduction of free volume upon increasing the crosslinking density, as seen in Figure 4. However, for membrane M-5, the observed permeation flux is more than that of the M-2 membrane throughout the range of feed composition, despite its higher crosslinking density compared to membranes M-2 to M-4. The effect of this can also be clearly viewed by plotting the total flux versus mass ratio of TEOS content in the membranes at 10 mass % of water in the feed, as shown in Figure 9. This unusual behavior may be due to the fact that at higher crosslinking density, the membrane loses its hydrophilic character considerably. In addition, the topology of this membrane may be such that the mesh size of the polymeric network and the diameter of the diffusion molecules are of the same order.[32] As a result, membrane M-5 apparently acts like a sieve and thereby the rate of permeation increased under the influence of vacuum on the downstream side of the membrane.

To differentiate the extent of permeation of individual components, we plotted the total flux and fluxes of water and isopropanol as a function of mass ratios of TEOS in the membranes for 10 mass % of water in the feed, as shown in Figure 10. From the plot it is observed that the magnitudes of total flux and flux of water are almost same except for lower and higher crosslinked membranes. This is because of greater swelling and loss of hydrophilic property at lower and higher crosslinking density, respectively. These led to the simultaneous permeation of isopropanol and water. But still, the permeation of isopropanol is negligible, suggesting that the membranes in the present study are highly water selective throughout the range of water content in the feed. However, membrane M-5 did not allow the permeation of isopropanol to a greater extent, even though the pore size of the membrane (M-5) and the diameter of the diffusing molecules are of the same order as observed in Figure 9. This may be due to the fact that the size of the water molecules (29.9 Å) is much smaller than that of isopropanol molecules (127.6 Å) and, hence, the membrane preferentially allowed the water molecules to permeate through sieving action to a greater extent.

Figure 11 displays the effect of water composition on the selectivity for all membranes. It is observed that the selectivity decreased drastically for all membranes up to 20 mass % of water and then it remains almost constant over the entire composition of water in the feed mixture, showing not much variation beyond 20 mass % of water in the feed. Calculated results of total flux and selectivity and fluxes of water and isopropanol, measured at 30°C for different compositions of

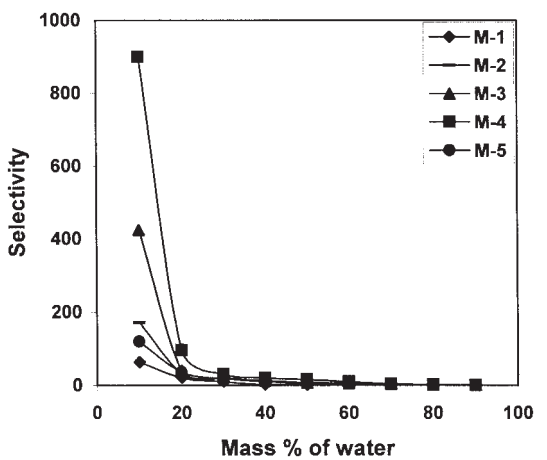

Figure 11 Variation of separation selectivity with different mass % of water in the feed at 30°C for different hybrid membranes.

TABLE I
Pervaporation Flux and Separation Selectivity Data for Different Membranes at 30°C for Different Mass % of Water in the Feed Mixture

Mass % of water	$J_p \times 10^2$ (kg/m^2 h)					α_{sep}				
	M-1	M-2	M-3	M-4	M-5	M-1	M-2	M-3	M-4	M-5
10	3.50	2.31	1.19	0.92	3.75	63.00	171.00	424.33	900.00	119.58
20	22.71	6.87	6.24	4.78	12.63	21.00	32.36	40.44	96.00	36.20
30	26.61	11.78	10.09	8.51	16.43	10.63	18.88	21.48	31.00	18.88
40	32.01	20.52	13.71	11.01	25.61	2.55	10.50	12.14	19.93	13.50
50	82.34	27.14	20.13	16.20	31.23	1.86	6.69	7.33	15.67	7.33
60	—	35.44	31.28	29.13	40.15	—	3.78	5.00	10.45	6.00
70	—	45.68	38.00	34.52	49.31	—	2.43	5.14	6.71	3.86
80	—	50.11	44.04	40.97	55.23	—	1.42	2.53	3.02	2.25
90	—	56.69	52.20	48.99	59.87	—	1.00	2.11	2.77	1.00

feed mixture with respect to mass ratios of TEOS in the membranes (M-1 to M-5), are presented in Tables I and II, respectively.

Diffusion coefficient

Transport of molecules in PV experiments has been explained by the solution-diffusion model.[33] Diffusion occurs as a result of concentration gradient as well as the driving force applied across the membrane. Therefore, it is important to estimate the diffusion coefficient, D_i, of solvent molecules to understand the transport mechanism. From the PV results, we have calculated D_i using the equation[34]

$$J_i = P_i[P_{i(feed)} - P_{i(permeate)}] = \frac{D_i}{h}[C_{i(feed)} - C_{i(permeate)}]. \quad (5)$$

Here, D_i is assumed to be constant across the effective membrane thickness, h; $C_{i(feed)}$ and $C_{i(permeate)}$ are, respectively, the concentration of water or IPA in the feed and permeate. The computed values of D_i (where subscript i stands for water or IPA) at 30°C are presented in Table III. As expected, the diffusion coefficients of water as well as IPA decrease from membrane M-1 to M-4, due to a reduction of free volume with increasing crosslinking density. However, there is a considerable increase in diffusion coefficients for all membranes in both cases with increasing the amount of water in the feed. Such an increase is quite dramatic at higher composition of water in the feed due to enhanced membrane swelling. Similar trends are observed for membrane M-5 with increasing water content in the feed, but its D_i values increased considerably instead of decreasing, even though the membrane has the highest crosslinking density. The unusual behavior of this membrane is a clear indication of the sieving action as observed in Figures 8 and 9.

Effect of temperature

To study the effect of temperature on PV performances for the water–isopropanol mixture, only suitable membranes were chosen for the feed mixture containing 10 mass % water. The results of PV flux and separation selectivity data at 30, 40, and 50°C are presented in Table IV. With increasing temperature, the values of flux increased and separation selectivity

TABLE II
Pervaporation Fluxes of Water and Isopropanol for Different Membranes at 30°C for Different Mass % of Water in the Feed Mixture

Mass % of water	$J_w \times 10^2$ (kg/m^2 h)					$J_{IPA} \times 10^2$ (kg/m^2 h)				
	M-1	M-2	M-3	M-4	M-5	M-1	M-2	M-3	M-4	M-5
10	3.19	2.19	1.16	0.91	3.45	0.31	0.12	0.03	0.01	0.30
20	19.08	5.81	5.62	4.59	11.36	3.63	1.06	0.62	0.19	1.27
30	21.82	10.48	9.10	7.91	14.62	4.79	1.30	0.99	0.60	1.81
40	23.17	18.02	12.13	10.24	23.05	8.84	2.50	1.58	0.77	2.56
50	53.52	23.61	17.71	15.23	27.48	28.82	3.53	2.42	0.97	3.75
60	—	30.12	28.15	26.22	36.13	—	5.32	3.13	2.91	4.02
70	—	38.83	34.58	31.48	44.38	—	6.85	3.42	3.04	4.93
80	—	42.59	39.53	37.31	49.71	—	7.52	4.51	3.66	5.52
90	—	51.02	47.50	44.07	53.88	—	8.67	4.70	4.92	5.99

TABLE III
Diffusion Coefficients of Water and Isopropanol for Different Membranes Calculated at 30°C from Eq. (5) for Different Mass % of Water in the Feed Mixture

Mass % of water	$D_w \times 10^5$ (cm^2/s)					$D_{IPA} \times 10^6$ (cm^2/s)				
	M-1	M-2	M-3	M-4	M-5	M-1	M-2	M-3	M-4	M-5
10	0.40	0.36	0.18	0.14	0.62	0.56	0.12	0.08	0.02	0.05
20	4.17	1.29	1.13	1.00	2.27	7.94	2.36	1.24	0.42	2.52
30	5.80	2.49	2.13	1.76	3.47	12.70	3.10	2.30	1.33	4.29
40	12.28	5.31	3.47	2.71	6.45	72.08	7.58	4.51	1.84	7.17
50	49.96	8.93	6.53	4.85	10.10	268.95	13.36	8.92	3.09	13.80
60	—	16.07	13.14	12.24	16.90	—	29.72	14.60	13.58	18.70
70	—	36.24	26.38	20.79	31.10	—	63.93	22.80	20.08	34.50
80	—	119.00	56.76	47.44	69.60	—	211.00	64.76	46.96	77.30
90	—	643.16	554.17	315.49	628.60	—	795.20	548.33	274.40	698.84

decreased systematically. This suggests that with increasing temperature the interactions between the water molecules, and the permeants and membrane become weaker, so that the plasticizing effects become more important.[35] As a result, the transport of water molecules facilitates along with IPA, while reducing the selectivity.

The temperature dependence of the permeation flux was therefore studied using the Arrhenius-type relation:

$$J_p = J_{p_o} \exp\left[\frac{-E_p}{RT}\right]. \quad (6)$$

Here, J_{p_0} and E_p are, respectively, pre-exponential factor and activation energy for permeation; R is the gas constant, and T is the temperature in degrees Kelvin. If the activation energy is positive, then the permeation flux increases with increasing temperature and this is indeed the case in most of the PV experiments.[8,36] Apart from the enhanced permeation flux, the driving force for mass transport also increases with increasing temperature. This driving force represents the concentration gradient resulting from a difference in the partial vapor pressure of the permeants between the feed and permeating mixture. As the feed temperature increases, the vapor pressure in the feed compartment also increases, but the vapor pressure at the permeate side is not affected. This leads to an increase of driving force due to an increase in temperature. In a similar way, mass transport due to diffusion was also calculated using the Arrhenius-type equation,

$$D = D_o \exp\left[\frac{-E_D}{RT}\right], \quad (7)$$

where D_o and E_D represent the pre-exponential factor and activation energy for diffusion, respectively.

The Arrhenius plots of log J_p versus $1/T$ and log D versus $1/T$ are shown in Figures 12 and 13 for temperature dependence of total permeation flux and diffusion, respectively. In both cases linear behavior is observed, signifying that temperature dependence of total permeation flux and diffusivity follows the Arrhenius trend. From a least-square fit of these linear plots, the activation energy values for total permeability (E_p) and diffusivity (E_D) were estimated and these were presented in Table V. The values of E_p and E_D are close to each other in each membrane, suggesting that both permeation and diffusion contribute almost equally to the PV process. The E_p and E_D values varied from 49.18 to 64.96 and 55.13 to 67.31 kJ/mol, respec-

TABLE IV
Pervaporation Flux and Separation Selectivity for Different Membranes at Different Temperatures for 10 Mass % of Water in the Feed Mixture

Temperature (°C)	$J_p \times 10^2$ (kg/m^2 h)			α_{sep}		
	M-2	M-3	M-4	M-2	M-3	M-4
30	2.31	1.19	0.92	171	424	900
40	4.25	2.88	1.78	81	103	141
50	7.73	5.16	4.55	51	81	125

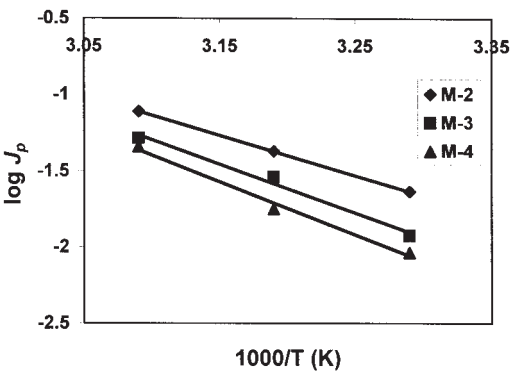

Figure 12 Variation of log J_p with temperature for 10 mass % of water in the feed.

tively. Using these values, we have further calculated the heat of sorption as

$$\Delta H_s = E_p - E_D. \quad (8)$$

The resulting ΔH_s values are included in Table V. These values are negative for the membranes studied, suggesting that Langmuir's sorption is still predominant, giving an exothermic contribution.

CONCLUSION

Hybrid membranes were prepared using PVA and TEOS through hydrolysis followed by cocondensation reaction and showed a significant improvement in the membrane performance while separating water–isopropanol mixtures. The separation factor increased profoundly upon increasing the crosslinking density (M-1 to M-4) due to a reduction of free volume and increased chain stiffness. However, the separation factor decreased drastically when PVA was crosslinked with the highest amount of TEOS (mass ratio of TEOS to PVA is 2:1). This unusual behavior was explained on the basis of considerable loss of hydrophilic character as well as on the topology of the polymer membrane. The highest separation selectivity is found to be 900 for M-4 at 30°C. For all membranes, the selectivity decreased drastically up to 20 mass % of water in the feed and then remained almost constant beyond 20 mass %, signifying that the separation selectivity is much influenced at lower composition of water in the feed. The PV separation index data also indicated that higher the degree of crosslinking, the better the membrane performance up to the maximum extent of 1.5:1 mass ratio of TEOS to PVA. On the other hand, permeation flux and swelling behavior increased linearly with increasing concentration of water in the feed due to an increase of selective interaction between the water molecules and hydrophilic membrane. As a result, transport of water molecules occurs across the membrane through easier diffusion.

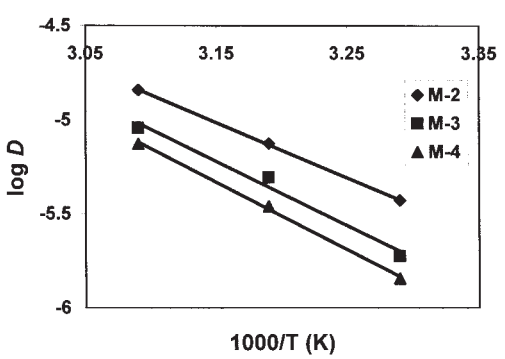

Figure 13 Variation of log D with temperature for 10 mass % of water in the feed.

TABLE V
Arrhenius Activation Parameters for Permeation and Diffusion and Heat of Sorption

Parameters	M-2	M-3	M-4
E_P (kJ/mol)	49.18	59.86	64.96
E_D (kJ/mol)	55.13	64.13	67.31
ΔH_s (kJ/mol)	−5.95	−4.27	−2.35

The estimated E_p and E_D values ranged from 49.18 to 64.96 and 55.13 to 67.31 kJ/mol, respectively. The small difference observed between E_p and E_D values, indicating that both permeation and diffusion contribute almost equally to the PV process. For all membranes, Langmuir's mode of sorption dominates the process, giving an exothermic contribution.

The authors thank Dr. M. K. Rabinal, Department of Physics, Karnatak University, Dharwad, for his valuable assistance in recording the X-ray patterns.

References

1. Yeom, C. K.; Huang, R. Y. M. J Membr Sci 1992, 67, 39.
2. Yoshikawa, M.; Yukoshi, T.; Sanui, K.; Ogata, N. J. Polym Sci Polym Chem Ed 1984, 24, 1585.
3. Sun, F.; Ruckenstein, E. J Membr Sci 1995, 99, 273.
4. Cabasso, I.; Grodzinski, J. G.; Vofsi, D. J Appl Polym Sci 1974, 18, 2137.
5. Duval, J. M.; Folkers, B.; Mulder, M. H. V.; Desgrandchamps, G.; Smolders, C. A. Sep Sci Technol 1994, 29, 357.
6. Mulder, M. H. V.; Krutiz, F.; Smolders, C. A. J Membr Sci 1982, 11, 349.
7. Nam, S. Y.; Chun, H. J.; Lee, Y. M. J Appl Polym Sci 1999, 72, 241.
8. Burshe, M. C.; Netke, S. A.; Sawant, S. B.; Joshi, J. B.; Pangarkar, V. G. Sep Sci Technol 1997, 32, 1335.
9. Ohya, H.; Matsumoto, K.; Negishi, Y.; Hino, T.; Choi, H. S. J Membr Sci 1992, 68, 141.
10. Huang, R. Y. M.; Jarvis, N. R. J Appl Polym Sci 1970, 14, 2341.
11. Shantora, V.; Huang, R. Y. M. J Appl Polym Sci 1981, 26, 3223.
12. Satoh, M.; Zhang, W. Z.; Nodera, A.; Komoyama, J. J Membr Sci 1988, 35, 311.
13. Huang, R. Y. M.; Shieh, J. J. J Appl Polym Sci 1998, 70, 317.
14. Sptizen, J. W. K. Ph. D. dissertation; Twente University: The Netherlands, 1988.
15. Nobrega, R.; Habert, A. C.; Esposito, M. E. F.; Borges, C. P. Proceedings of the 3rd International Conference on Pervaporation Processes in the Chem Industry, R. Bakish, Ed.; Bakish Material Corp.: Englewood, NJ, 1988; p. 326.
16. Korsmeyer, R. W.; Peppas, N. A. J Membr Sci 1981, 9, 211.
17. Ying, W. Desalination 1983, 46, 335.
18. Katz, M. G.; Wydeven, T. Jr. J Appl Polym Sci 1981, 26, 2935.
19. Katz, M. G.; Wydeven, T. Jr. J Appl Polym Sci 1982, 27, 79.
20. Hirotsu, T.; Ichimura, K.; Mizoguch, K.; Nakamura, E. J Appl Polym Sci 1988, 36, 1717.
21. Feng, Q.; Xu, J.; Dong, H.; Li, S.; Wei, Y. J Mater Chem 2000, 10, 2490.
22. Ismail, A. F.; David, L. I. B. J Membr Sci 2001, 193, 1.
23. Kim, K. J.; Park, S. H.; So, W. W.; Moon, S. J. J Appl Polym Sci 2001, 79, 1450.
24. Uragami, T.; Okazaki, K.; Matsugi, H.; Miyata, T. Macromolecules 2002, 35, 9156.

25. Bellamy, N. J. The Infrared Spectra of Complex Molecules; Chapman and Hall: London, 1975; p. 378.
26. Robertson, M. A. F.; Mauritz, K. A. J Polym Sci B Polym Phys 1998, 36, 595.
27. Carraher, C. E. Jr.; Pittman, C. U. Jr. Industrial Polymers Handbook, Wiley-VCH: Weinheim, 2001; p. 1284.
28. Kittur, A. A.; Kariduraganavar, M. Y.; Toti, U. S.; Ramesh, K.; Aminabhavi, T. M. J Appl Polym Sci 2003, 90, 2441.
29. Burshe, M. C.; Sawant, S. B.; Joshi, J. B.; Pangarkar, V. G. Sep Purif Technol 1997, 12, 145.
30. Flory, P. J. Principles of Polymer Chemistry; Cornell University Press: Ithaca, NY, 1953; p. 509.
31. Flory, P. J.; Rehner, J. Jr. J Chem Phys 1943, 11, 521.
32. Moynihan, H. J.; Peppas, N. A. Polym News 1984, 9, 236.
33. Binning, R. C.; Lee, R. J.; Jennings, J. F.; Martin, E. C. Ind Eng Chem 1961, 53, 45.
34. Kusumocahyo, S. P.; Sudoh, M. J Membr Sci 1999, 161, 77.
35. Wang, Y. H.; Teng, M.Y.; Lee, K. R.; Wang, D. M.; Lai, J. Y. Sep Sci Technol 1998, 33, 1653.
36. Nam, S. Y.; Lee, Y. M. J Membr Sci 1999, 157, 63.